Award Number: W81XWH-20-1-0335

TITLE: Immunotherapy Targeting Stromal CD5L in Ovarian Cancer

PRINCIPAL INVESTIGATOR: Yunfei Wen

CONTRACTING ORGANIZATION: The University of Texas MD Anderson Cancer Center

REPORT DATE: Oct 2023

TYPE OF REPORT: Annual

PREPARED FOR: U.S. Army Medical Research and Development Command
Fort Detrick, Maryland 21702-5012

DISTRIBUTION STATEMENT: Approved for Public Release;
Distribution Unlimited

REPORT DOCUMENTATION PAGE		Form Approved OMB No. 0704-0188
Public reporting burden for this collection of information is estimated to average 1 hour per response, including the time for reviewing instructions, searching existing data sources, gathering and maintaining the data needed, and completing and reviewing this collection of information. Send comments regarding this burden estimate or any other aspect of this collection of information, including suggestions for reducing this burden to Department of Defense, Washington Headquarters Services, Directorate for Information Operations and Reports (0704-0188), 1215 Jefferson Davis Highway, Suite 1204, Arlington, VA 22202-4302. Respondents should be aware that notwithstanding any other provision of law, no person shall be subject to any penalty for failing to comply with a collection of information if it does not display a currently valid OMB control number. **PLEASE DO NOT RETURN YOUR FORM TO THE ABOVE ADDRESS.**		
1. REPORT DATE Oct 2023	**2. REPORT TYPE** ANNUAL	**3. DATES COVERED** 1SEPT2022-31AUG2023
4. TITLE AND SUBTITLE Immunotherapy Targeting Stromal CD5L in Ovarian Cancer		**5a. CONTRACT NUMBER** W81XWH-20-1-0335
		5b. GRANT NUMBER
		5c. PROGRAM ELEMENT NUMBER
6. AUTHOR(S) Yunfei Wen E-Mail:ywen2@mdanderson.org		**5d. PROJECT NUMBER** **5e. TASK NUMBER** **5f. WORK UNIT NUMBER**
7. PERFORMING ORGANIZATION NAME(S) AND ADDRESS(ES) **AND ADDRESS(ES)** The University of Texas MD Anderson Cancer Center		**8. PERFORMING ORGANIZATION REPORT NUMBER**
9. SPONSORING / MONITORING AGENCY NAME(S) AND ADDRESS(ES) U.S. Army Medical Research and Development Command Fort Detrick, Maryland 21702-5012		**10. SPONSOR/MONITOR'S ACRONYM(S)** **11. SPONSOR/MONITOR'S NUMBER(S)**
12. DISTRIBUTION / AVAILABILITY STATEMENT Approved for Public Release; Distribution Unlimited		
13. SUPPLEMENTARY NOTES		

14. ABSTRACT

Although the FDA approved anti-angiogenesis therapies, such as bevacizumab, for treatment in upfront and relapsed ovarian cancers, the development of adaptive resistance to such therapy remains a major clinical barrier. To date, only a portion of the molecular mechanisms underlying drug resistance to anti-VEGF antibody therapy like bevacizumab have been studied. The proposed work aims to investigate the therapeutic potential for a novel monoclonal antibody, rAb-anti-CD5L to overcome adaptive resistance in ovarian cancer during application of anti-VEGF drugs. We also aim to characterize the roles for CD5L and its endothelial-specific receptors in mediating development of resistance to anti-VEGF antibody therapeutics in endothelial cells, and the mechanisms of rAb-anti-CD5L in interfering with such activities. The *short-term goal* of this proposal is to understand mechanisms of action of rAb-anti-CD5L in targeting stromal CD5L in ovarian tumors with anti-VEGF-therapy resistance. We expect this work will lead to a new therapeutic approach for ovarian cancer patients. Overall, our proposal is highly translational and has profound implications for developing a novel, antibody-based therapy for ovarian cancer. Thus, this proposal is directly responsive to the Program Announcement for the Investigator-Initiated Research Award from DOD-OCRP, in that we will identify novel approaches for overcoming adaptive resistance to anti-VEGF therapy in ovarian cancer. Further clinical development of rAb-anti-CD5L will require formal safety studies (GLP regulations); we are well poised to carry out such work and have extensive experience in drug development. As the future effort, we will take advantage of the Moonshot Program for Ovarian Cancer at MD Anderson, which will provide clinical resources for us to formally test the utility of anti-CD5L antibody-based drugs to overcome the adaptive resistance developed from anti-angiogenic therapy including bevacizumab.

15. SUBJECT TERMS

Therapeutic, Adaptive resistance

16. SECURITY CLASSIFICATION OF:	**17. LIMITATION OF ABSTRACT**	**18. NUMBER OF PAGES**	**19a. NAME OF RESPONSIBLE PERSON** USAMRDC

a. REPORT	b. ABSTRACT	c. THIS PAGE			19b. TELEPHONE NUMBER *(include area code)*
U	U	U	UU	20	

Prescribed by ANSI Std. Z39.18

TABLE OF CONTENTS

Introduction

Anti-angiogenesis therapy using the monoclonal anti-VEGF antibody bevacizumab is an efficacious treatment of advanced ovarian cancer in either the maintenance or recurrent setting – for which it has FDA approval. Unfortunately, the majority of women treated with this drug will eventually develop resistance, leading to subsequent recurrence or progression of disease. Therefore, new and effective approaches are needed to avoid or reverse adaptive resistance to bevacizumab treatment. Previous unpublished work from our laboratory identified markedly elevated levels of CD5L in tumor endothelial cells related to emergence of adaptive resistance to anti-VEGF therapy. ***Our central hypothesis is that in addition to interfering with the known effects of CD5L on macrophages, rAb-anti-CD5L will overcome adaptive resistance to anti-VEGF therapy by targeting tumor vasculature.*** This hypothesis is based on our findings that decreasing the activity of CD5L – whether from an mRNA or protein level – leads to improved sensitivity to anti-VEGF therapy. Our team includes leading experts in ovarian cancer biology, angiogenesis pathways, developmental therapeutics, and the care of women with ovarian cancer. Furthermore, our laboratory has published multiple previous studies involving the complete derivation of cellular pathways and the phenotypic effect of pathway disruptions using *in vivo* animal models. Therefore, these factors have placed us in an excellent position to carry out the proposed study. In this proposal, we will test our central hypothesis under the following aims:

Specific Aims: #**1**: **Evaluate the therapeutic efficacy of rAb-anti-CD5L in overcoming adaptive resistance to anti-VEGF therapy using cell-based and patient-derived xenograft orthotopic ovarian cancer models**; We will use our established syngeneic and orthotopic (e.g., ID8) mouse models of ovarian cancer and ovarian cancer patient-derived xenograft models. The effects of rAb-anti-CD5L will be tested in these ovarian cancer models, as well as in those with adaptive resistance to AVA therapy. Renal and liver toxicities of the rAb-anti-CD5L antibody will be addressed by measuring the creatinine and liver function tests pre- and post-treatment. The stromal effects of rAb-anti-CD5L will be assessed with immunohistologic analysis in the resulting tumors.

Specific Aims: #**2**: **Determine the mechanisms by which rAb-anti-CD5L reduces resistance to anti-VEGF therapy in endothelial cells.** ***Study Design***: We will first functionally characterize the endothelial-specific, cell-membrane receptors binding to stromal CD5L and mediating the angiogenic signaling. Second, we will determine the potential factors/mechanisms for upregulating CD5L in addition to PPAR-γ, an upstream factor of CD5L in promoting AVA resistance and hypoxia. Thirdly, we will also perform protein profiling using reverse phase protein arrays (RPPA) and angiogenic array to identify downstream factors for rAb-anti-CD5L treatment in endothelial cells with bevacizumab resistance. Lastly, we will investigate the mechanical effect of rAb-anti-CD5L on autophagy and angiogenic properties in endothelial cells.

Keywords

Ovarian cancer, CD5L, therapeutic antibody, adaptive resistance

Accomplishments

Aim 1: Evaluate the therapeutic efficacy of rAb-anti-CD5L in overcoming adaptive resistance to anti-VEGF therapy using cell-based and patient-derived xenograft orthotopic ovarian cancer models.

Major task 1a: Investigate the effect of rAb-anti-CD5L using syngeneic and orthotopic nude mouse models of ovarian cancer with adaptive resistant to AVA therapy.

- *Subtask 1a-1: Submit documents for local IACUC and IRB review;*

Previous reports: All amendments proposed in this study have been submitted to the institution's IACUC and gained the approvals including using orthotopic, syngeneic ovarian cancer cell-based models, and high-grade ovarian cancer patient xenograft derived models for testing our rAb-anti-CD5L antibodies R35 (intraperitoneal or subcutaneous tumor injection). IACUC protocol (00001029-RN03). In addition, the protocol was approved by Animal Care and Use Review Office (ACURO) in March 2021. We received exemption from HRPO approval or exemption from human subjects/HAS related studies on April 17, 2021.

In addition, to establish the syngeneic and orthotopic nude mouse models of ovarian cancer with adaptive resistance to AVA therapy, we have submitted the proposal titled as “Effect of CD5L inhibition on growth and survival of ovarian/endometrial cancer models” to Genentech, Inc and requested anti-human VEGF-A antibody Bevacizumab and the anti-human/mouse VEGF-A antibody B20 4.1.1. This MTA has been processed and approved in July 2021.

- *Subtask 1a-2: Investigate the effect of rAb-anti-CD5L using syngeneic and orthotopic nude mouse models of ovarian cancer with adaptive resistance to AVA therapy.*

Overview: Given our preliminary data showed that AVA resistance is mediated, in part, by overexpression of CD5L, we have tested an antibody to specifically target CD5L, named as rAb-anti-CD5L (aka, CD5L-R35mAb) and the isotype control IgG (Rab57.4). Our goal in this subtask is to investigate the therapeutic potential and mechanisms for rAb-anti-CD5L for the following two purposes: A) as monotherapy or in combination with paclitaxel; B) for overcoming adaptive resistance to anti-angiogenesis in syngeneic HGSC mouse models of luciferase-labeled ID8 or in orthotopic HGSC models of OVCA8-luciferase using athymic nude mice. In here, we have used the syngeneic ID8$^{KO\text{-}Trp53;Brca2}$ tumor models in this subtask for the reason that, in comparing with ID8 WT cells, ID8$^{KO\text{-}Trp53;Brca2}$ is reported to have high genomic instability, which is a common feature of HGSC (Walton et al., 2016). We hypothesize that in addition to interfering with the known effects of CD5L on macrophages, rAb-anti-CD5L will overcome adaptive resistance to anti-VEGF therapy by targeting tumor vasculature. We propose the following experimental procedures for testing this hypothesis (Figure 1).

Figure 1. Schematic representations of the mouse models were established using a metastatic model of ID8$^{KO\text{-}Trp53;Brca2}$ or OVCAR8- IP2 models labeled with luciferase (OVCA8-Luc-ip2 4x10^6/mouse). A&B: Therapeutic experiment for rAb-anti-CD5L and chemotherapy study in OVCAR8-Luc-IP2 or ID8$^{KO\text{-}Trp53;Brca2}$ models. C&D: Establishing adaptive resistance in orthotopic ovarian cancer models and the treatment strategy of rAb-anti-5L using OVCAR8-Luc-IP2 or ID8$^{KO\text{-}Trp53;Brca2}$ models.

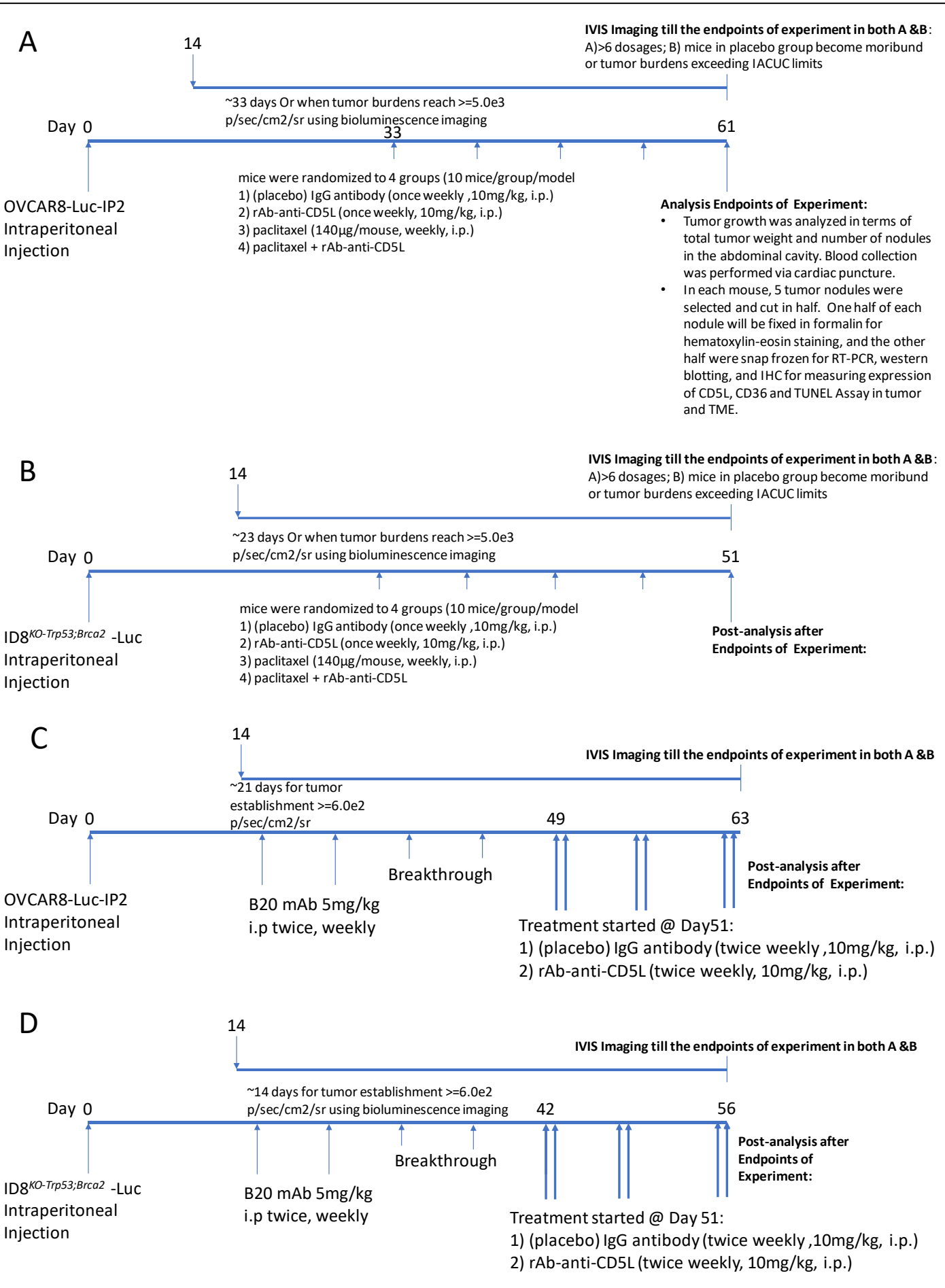
A
14
IVIS Imaging till the endpoints of experiment in both A &B:
A)>6 dosages; B) mice in placebo group become moribund or tumor burdens exceeding IACUC limits
~33 days Or when tumor burdens reach >=5.0e3 p/sec/cm2/sr using bioluminescence imaging
Day 0
33
61
OVCAR8-Luc-IP2 Intraperitoneal Injection
mice were randomized to 4 groups (10 mice/group/model
1) (placebo) IgG antibody (once weekly ,10mg/kg, i.p.)
2) rAb-anti-CD5L (once weekly, 10mg/kg, i.p.)
3) paclitaxel (140μg/mouse, weekly, i.p.)
4) paclitaxel + rAb-anti-CD5L
Analysis Endpoints of Experiment:
• Tumor growth was analyzed in terms of total tumor weight and number of nodules in the abdominal cavity. Blood collection was performed via cardiac puncture.
• In each mouse, 5 tumor nodules were selected and cut in half. One half of each nodule will be fixed in formalin for hematoxylin-eosin staining, and the other half were snap frozen for RT-PCR, western blotting, and IHC for measuring expression of CD5L, CD36 and TUNEL Assay in tumor and TME.
B
14
IVIS Imaging till the endpoints of experiment in both A &B:
A)>6 dosages; B) mice in placebo group become moribund or tumor burdens exceeding IACUC limits
~23 days Or when tumor burdens reach >=5.0e3 p/sec/cm2/sr using bioluminescence imaging
Day 0
51
ID8KO-Trp53;Brca2 -Luc Intraperitoneal Injection
mice were randomized to 4 groups (10 mice/group/model
1) (placebo) IgG antibody (once weekly ,10mg/kg, i.p.)
2) rAb-anti-CD5L (once weekly, 10mg/kg, i.p.)
3) paclitaxel (140μg/mouse, weekly, i.p.)
4) paclitaxel + rAb-anti-CD5L
Post-analysis after Endpoints of Experiment:
C
14
IVIS Imaging till the endpoints of experiment in both A &B
~21 days for tumor establishment >=6.0e2 p/sec/cm2/sr
Day 0
49
63
Breakthrough
Post-analysis after Endpoints of Experiment:
OVCAR8-Luc-IP2 Intraperitoneal Injection
B20 mAb 5mg/kg i.p twice, weekly
Treatment started @ Day51:
1) (placebo) IgG antibody (twice weekly ,10mg/kg, i.p.)
2) rAb-anti-CD5L (twice weekly, 10mg/kg, i.p.)
D
14
IVIS Imaging till the endpoints of experiment in both A &B
~14 days for tumor establishment >=6.0e2 p/sec/cm2/sr using bioluminescence imaging
Day 0
42
56
Breakthrough
Post-analysis after Endpoints of Experiment:
ID8KO-Trp53;Brca2 -Luc Intraperitoneal Injection
B20 mAb 5mg/kg i.p twice, weekly
Treatment started @ Day 51:
1) (placebo) IgG antibody (twice weekly ,10mg/kg, i.p.)
2) rAb-anti-CD5L (twice weekly, 10mg/kg, i.p.)

Results:

In the previous report, we tested the therapeutic efficacy of CD5L-35Rb and control antibody Rab57.4 antibodies in high-grade serous ovarian cancer (HGSC) model OVCAR8 in the therapeutic setting (CD5L-35Rb as monotherapy or in combination with the chemotherapeutic drug paclitaxel) and the anti-VEGF-A antibody adaptive resistance setting (Chen 2012).

Figure 2. Effects of rAb-anti-CD5L(CD5L-35Rb) on expression of CD5L/CD36 axis and death, as well as endothelial CD36 levels in OVCAR8_luc tumors

Mouse models were established using an orthotopic model of HGSC-OVCAR8 cells labeled with luciferase (OVCAR8-Luc-IP2-luc 1x10^6/mouse) via intraperitoneal injection. Mice were randomized into 4 groups (n>=7) after 33 days after tumor establishment, as confirmed by weekly bioluminescence (till tumor burden reach >=5.0e3 p/sec/cm2/sr). Then, the randomized animals are separated into 4 groups and treated with: 1) IgG (Rab57.4)-control, 2) rAb-anti-CD5L(CD5L-35Rb) at 10mg/kg, 3) paclitaxel 100mg/kg, or 4) combination of rAb-anti-CD5L(CD5L-35Rb) at 10mg/kg, paclitaxel 100mg/kg. We completed 4 dosages before the sacrifice of all animals at Day 61 after initial inoculation (the control group became moribund or reached the tumor size limits from IACUC). (A) Tumor weight, (B) number of nodules, (C) mouse body weight of each mouse were recorded at the time of necropsy.
(A) Tumor weight: IgG (Rab57.4)-control vs rAb-anti-CD5L(CD5L-35Rb), p=0.05; IgG (Rab57.4)-control vs paclitaxel 100mg/kg p=0.05, IgG (Rab57.4)-control vs rAb-anti-CD5L(CD5L-35Rb) + paclitaxel 100mg/kg p=0.005, determined by using a two-tailed, nonparametric *t*-test. Error bars represent SEM.
(B) Number of nodules: IgG (Rab57.4)-control vs rAb-anti-CD5L(CD5L-35Rb), p=0.03; IgG (Rab57.4)-control vs paclitaxel 100mg/kg p=0.02, IgG (Rab57.4)-control vs rAb-anti-CD5L(CD5L-35Rb) + paclitaxel 100mg/kg p=0.001, determined by using a two-tailed, nonparametric *t*-test. Error bars represent SEM.
(C) No significant differences were observed between each group.
(D) Upper: Representative immunofluorescence images showing expression of CD5L (Green), cell death marker cleaved caspase 3, and Hoechst as nucleus in tumor sections from each treatment group.
Bottom: Representative immunofluorescence images showing expression of CD36 (Green), cell death marker cleaved caspase 3, and Hoechst as nucleus in tumor sections from each treatment group. Scale bar = 50 μm.
Immunofluorescence in each image will be quantified measured by their fluorescence intensity with Imaris v.9.1.2. (Pending).
(E) Representative immunofluorescence images showing expression of CD36 (Green), endothelial cell marker CD31(Red), and Hoechst as nucleus in tumor sections from each treatment group.
Scale bar = 50 μm. Immunofluorescence in each image will be quantified measured by their fluorescence intensity with Imaris v.9.1.2. (Pending).

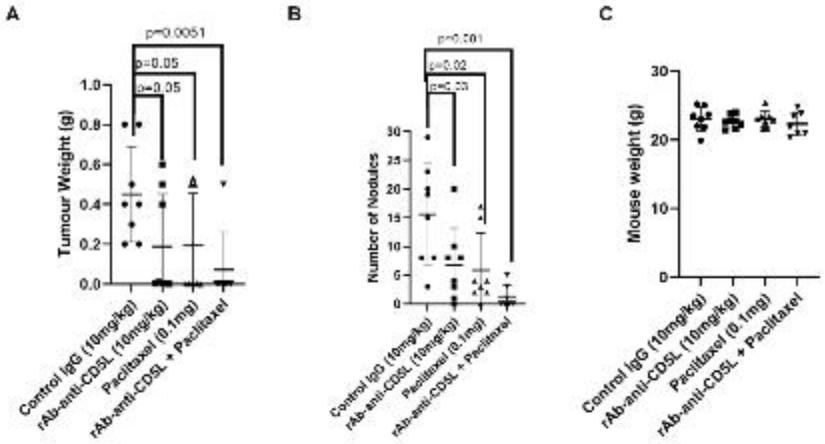

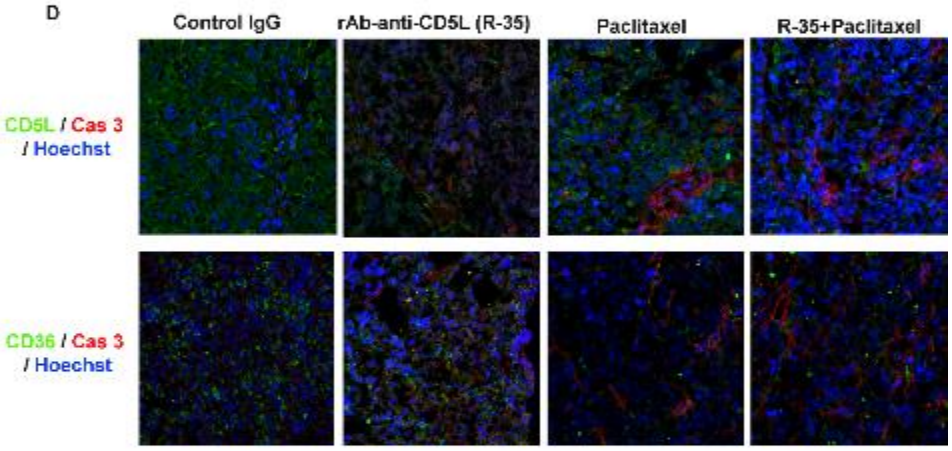

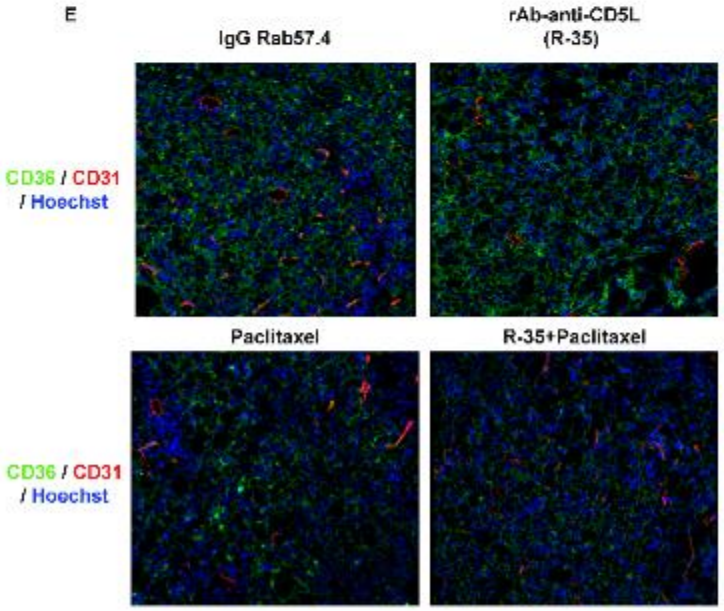

Conclusion: In HGSC model (OVCAR8-Luc-IP2-luc), mice treated with the IgG (Rab57.4)-control antibody had significantly larger tumor burden than those treated with rAb-anti-CD5L(CD5L-35Rb). The combination treatment of rAb-anti-CD5L(CD5L-35Rb) and paclitaxel has reduced the expression of CD5L and increased the levels of cleaved caspase-3, but did not change the membrane-receptor CD36 expression (Fig 2D). The levels of multivesicular

density represented by CD31 was decreased in rAb-anti-CD5L(CD5L-35Rb) monotherapy as well as in combination with paclitaxel.
The quantification of the fluorescence intensity in each group will be measured by Imaris v.9.1.2.

Next, we used the anti-human/mouse VEGF-A antibody B20 4.1.1. (MTA, GenenTech) to establish the orthotopic (OVCAR8-Luc-IP2) HGSC mouse models of ovarian cancer with adaptive resistance to AVA therapy (**Figure 3).**

Figure 3. Effect of rAb-anti-CD5L(CD5L-35Rb) on expression of CD5L/CD36 axis and death, as well as endothelial CD36 levels in OVCAR8-Luc-IP2 with adaptive resistant to AVA therapy (B20).
B20-adaptive resistant models were established using an orthotopic model of OVCAR8-Luc-IP2-luc 1x10⁶/mouse via intraperitoneal injection. At ~21 days after tumor establishment, as confirmed by weekly bioluminescence (till tumor burden reach >=6.0e2 p/sec/cm2/sr), all mice were receiving anti- VEGF-A antibody B20 5mg/kg bi-weekly via intraperitoneal injection. Approximately 4 weeks after B20 injection, when mice indicated the increases in tumor burden appear from previously stable disease (i.e., breakthrough, an indication of acquired resistance), the B20-resistant tumor bearing mice will be randomized into the following treatment groups: 1) IgG (Rab57.4)-control, 2) rAb-anti-CD5L(CD5L-35Rb) at 10mg/kg. Both were administrated via intraperitoneal injection bi-weekly.
We completed 4 dosages before the sacrifice of the 1st set of B20-adaptive resistant OVCAR8-Luc-IP2-luc animals, at the time points of the control group became moribund or reached the tumor size limits from IACUC.

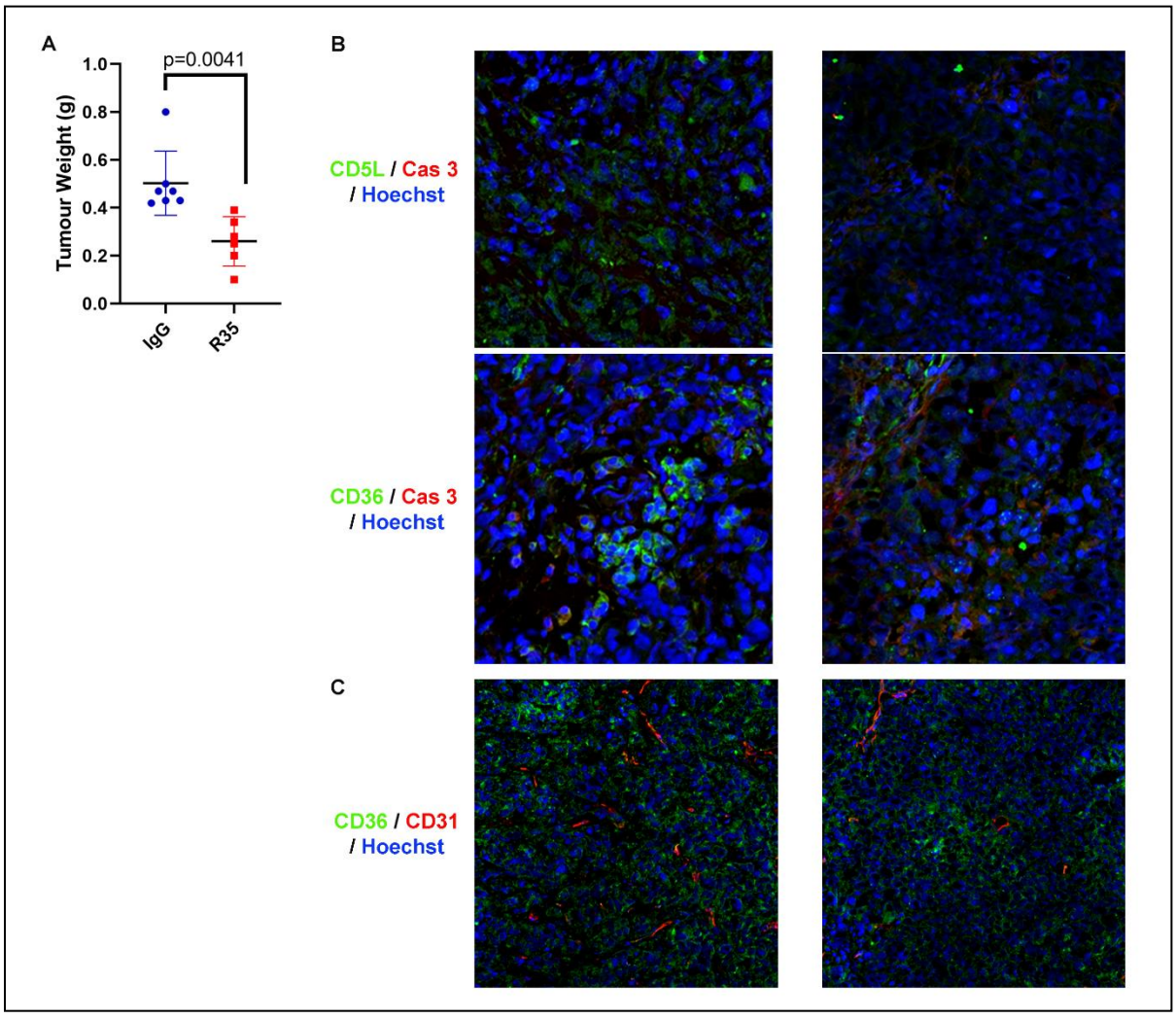

(A) Tumor weight of each mouse were recorded at the time of necropsy.
(B) Upper: Representative immunofluorescence images showing expression of CD5L (Green), cell death marker cleaved caspase 3, and Hoechst as nucleus in tumor sections from each treatment group.

Bottom: Representative immunofluorescence images showing expression of CD36 (Green), cell death marker cleaved caspase 3, and Hoechst as nucleus in tumor sections from each treatment group. Scale bar = 50 μm.

Immunofluorescence in each image will be quantified measured by their fluorescence intensity with Imaris v.9.1.2. (Pending).
(C) Representative immunofluorescence images showing expression of CD36 (Green), endothelial cell marker CD31(Red), and Hoechst as nucleus in tumor sections from each treatment group.
Scale bar = 50 μm. Immunofluorescence in each image will be quantified measured by their fluorescence intensity with Imaris v.9.1.2. (Pending).

Conclusion: In the OVCAR8-Luc-IP2-luc model with adaptive resistance to AVA therapy (B20), mice treated with the IgG (Rab57.4)-control antibody had significantly larger tumor burden than those treated with rAb-anti-CD5L(CD5L-35Rb). The rAb-anti-CD5L(CD5L-35Rb) treatment has reduced the expression of CD5L and increased the levels of cleaved caspase-3,but did not change the membrane-receptor CD36 expression (Fig 3B). The levels of multivesicular density represented by CD31 was decreased in rAb-anti-CD5L(CD5L-35Rb) as well (Fig 3C).
The quantification of the fluorescence intensity in each group will be measured by Imaris v.9.1.2.

Next, We have established syngeneic ID8$^{KO\text{-}Trp53;Brca2}$ -luc mouse models for the therapeutic experiments in combination with taxane-based drug paclitaxel, as well as the ID8$^{KO\text{-}Trp53;Brca2}$ models with adaptive resistant to AVA therapy (B20). The experimental strategies are described in Figure 1B and Figure 1D.

Figure 4. Effects of rAb-anti-CD5L(CD5L-35Rb) on therapeutic setting with paclitaxel and expression of CD5L/CD36 axis and death, as well as endothelial CD36 levels in syngeneic ID8$^{KO\text{-}Trp53;Brca2}$ -luc mouse model.
Mouse models were established using ID8$^{KO\text{-}Trp53;Brca2}$ -luc cells (1.5x10^{6}/mouse) via intraperitoneal injection. Mice were randomized into 4 groups (n>=7) after 33 days after tumor establishment, as confirmed by weekly bioluminescence (till tumor burden reach >=5.0e3 p/sec/cm2/sr). Then, the randomized animals are separated into 4 groups and treated with: 1) IgG (Rab57.4)-control, 2) rAb-anti-CD5L(CD5L-35Rb) at 10mg/kg, 3) paclitaxel 100mg/kg, or 4) combination of rAb-anti-CD5L(CD5L-35Rb) at 10mg/kg, paclitaxel 100mg/kg. We completed 6 dosages before the sacrifice of all animals at Day 61 after initial inoculation (the control group became moribund or reached the tumor size limits from IACUC). (A) Tumor weight, (B) number of nodules, (C) volume of body ascites, (D) mouse body weight of each mouse were recorded at the time of necropsy.
(A) tumor weight: rAb-anti-CD5L(CD5L-35Rb) monotherapy vs rAb-anti-CD5L(CD5L-35Rb) + paclitaxel 100mg/kg combination, P=0.0525 in determined by using a two-tailed, nonparametric *t*-test. Error bars represent SEM.
(E) Photographs of representative mouse from each group at the time of necropsy.
(F) Upper: Representative immunofluorescence images showing expression of CD5L (Green), cell death marker cleaved caspase 3, and Hoechst as nucleus in tumor sections from each treatment group.

Bottom: Representative immunofluorescence images showing expression of CD36 (Green), cell death marker cleaved caspase 3, and Hoechst as nucleus in tumor sections from each treatment group. Scale bar = 50 μm.

Immunofluorescence in each image will be quantified measured by their fluorescence

intensity with Imaris v.9.1.2. (Pending).

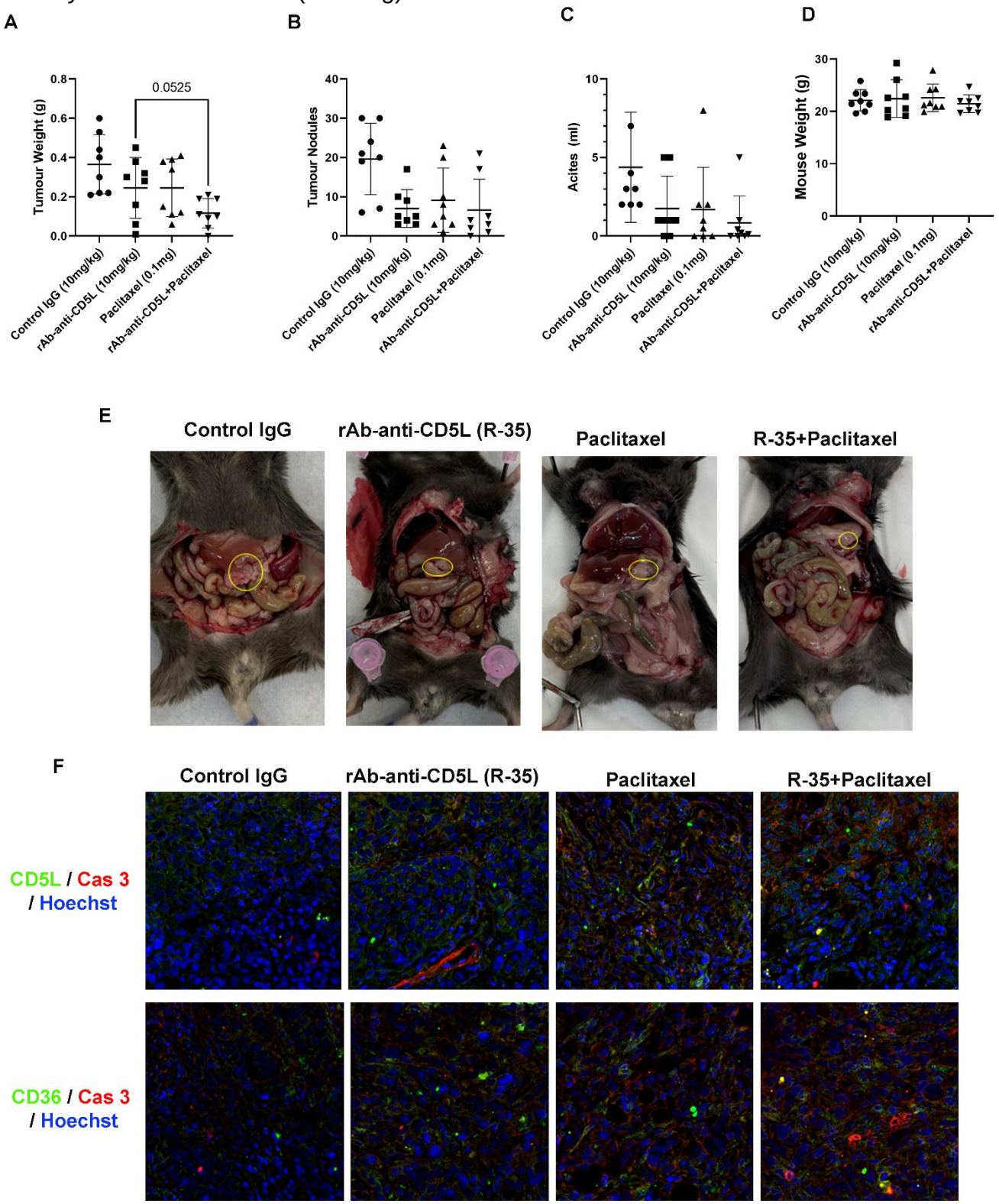

Conclusion: In immunocompetent ID8$^{KO\text{-}Trp53;Brca2}$ -luc model, mice treated with the IgG (Rab57.4)-control antibody had larger tumor burden than those treated with rAb-anti-CD5L(CD5L-35Rb), but the p value is not significant. The combination treatment of rAb-anti-

CD5L(CD5L-35Rb) and paclitaxel has reduced the tumor weight in comparison with the rAb-anti-CD5L(CD5L-35Rb) monotherapy (p=0.0525, Fig 4A-4D). The combination treatment also reduced the expression of CD5L and increased the levels of cleaved caspase-3, but did not change the membrane-receptor CD36 expression (Fig 4F).

The quantification of the fluorescence intensity in each group will be measured by Imaris v.9.1.2.

Figure 5. Effect of rAb-anti-CD5L(CD5L-35Rb) in decreasing tumor burden and inhibiting tumor growth in syngeneic ID8$^{KO\text{-}Trp53;Brca2}$ -luc mouse model with adaptive resistant to AVA therapy (B20).

B20-adaptive resistant models were established using ID8$^{KO\text{-}Trp53;Brca2}$ -luc cells ($1.5x10^6$/mouse) via intraperitoneal injection. At ~21 days after tumor establishment, as confirmed by weekly bioluminescence (till tumor burden reach >=6.0e2 p/sec/cm2/sr), all mice were receiving anti- VEGF-A antibody B20 5mg/kg bi-weekly via intraperitoneal injection. Approximately 6 weeks after B20 injection, when mice indicated the increases in tumor burden appear from previously stable disease (i.e., breakthrough, an indication of acquired resistance), the B20-resistant tumor bearing mice will be randomized into the following treatment groups: 1) IgG (Rab57.4)-control, 2) rAb-anti-CD5L(CD5L-35Rb) at 10mg/kg. Both were administrated via intraperitoneal injection bi-weekly. We completed 4 dosages before the sacrifice of the 1st set of B20-adaptive resistant ID8$^{KO\text{-}Trp53;Brca2}$ -luc animals, at the time points of the control group became moribund or reached the tumor size limits from IACUC.

(A &B) (Right) Bioluminescence images were shown for the last three doses of B20 given in each group and stopped when they developed “breakthrough”, afterwards, animals received (A) IgG (Rab57.4)-control at 10mg/kg or (B) rAb-anti-CD5L(CD5L-35Rb) at 10mg/kg for 4 doses. Continuation of bioluminescence images were recorded before takedown. Auto exposure was applied in each acquisition during imaging. Once all time points and all mice have been imaged, we returned to the imaging station and adjusted the color scale gating to be consistent across all images (Min=3.00e3/Max=5.50e4). This adjustment leaves the underlying photon counts unchanged and allows us to quantitatively compare all images across time points and mice.

(C) Tumor weight, (D) number of nodules, (E) volume of body ascites (F) mouse body weight of each mouse was recorded at the time of necropsy. P values were determined by using a two-tailed, nonparametric *t*-test. Error bars represent SEM.

(G) Total counts of bioluminescence were graphed starting Day 21 (B20-injection) to show the tumor growth progression.

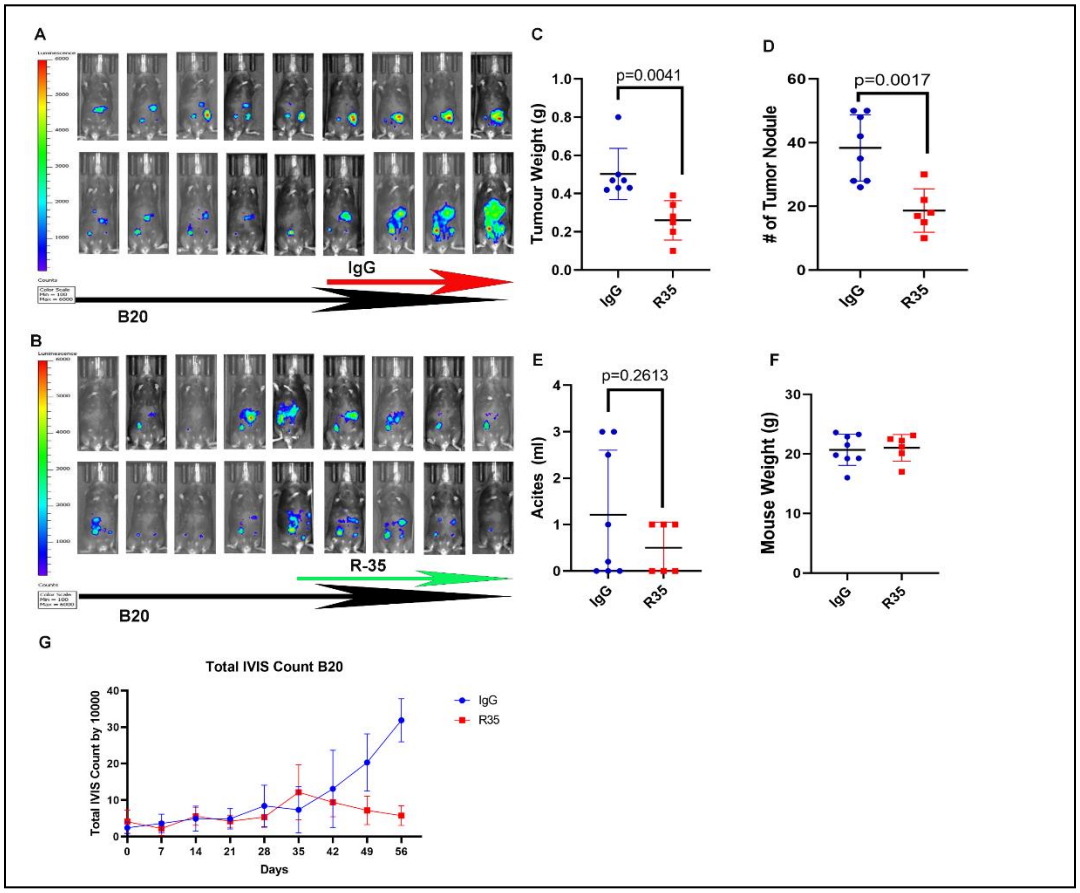

- *<u>Subtask 1a-3:</u> Investigate the effect of rAb-anti-CD5L in orthotopic mouse models of OVCA. 432-luc model with adaptive resistance to B20.*

The orthotopic nude mouse models of ovarian cancer (OVCA-432-luciferase) with adaptive resistance to B20 anti-VEGF-A antibody is ongoing.

Major task 1b: Determine the stromal effects of rAb-anti-CD5L in the AVA-resistant tumors.

- <u>Subtask 1b-1</u>: Test the hypoxia effect in *rAb-anti-CD5L* treated orthotopic and syngeneic ovarian tumors with adaptive resistance to AVA therapy.
  The hypoxia levels of B20-adaptive resistant tumors in ID8$^{KO\text{-}Trp53;Brca2}$ -luc and OVCAR8-Luc models affected by rAb-anti-CD5L is ongoing.
- <u>Subtask 1b-2</u>: immunohistochemical (IHC) analysis using antibodies for proliferation (Ki67), angiogenesis represented by microvascular density (MVD) with CD31, and apoptosis (TUNEL);
  We have completed the staining with proliferation (Ki67), angiogenesis represented by microvascular density (MVD) with CD31, and apoptosis (cleaved caspase -3) in the resulting tumors of therapeutic setting (Arm A) and AVA-resistant setting (Arm B). We will quantify the fluorescence intensity with Imaris v.9.1.2 to get the statistic results.
- <u>Subtask 1b-3</u>: Compare the expression of CD5L/CD36 axis on macrophage using F4/80 co-staining with flow cytometry;
  This experiment is ongoing.

- Subtask 1b-4: Profile other immune cell populations (MDSCs, DC, T-regs, CD4/8 cells, and NK cells) by co-immunofluorescence staining and by CyTOF system in the resulting tumors.

  This experiment is ongoing.

Major task 1c: Determine the effects of rAb-anti-CD5L in the AVA-resistant PDX models from high-grade serous ovarian cancer (HGSC) patients.

We have established the HGSC PDX models (#2428 and #2414), and the donor mice are currently under the way for establish the tumors. The therapeutic experiment will be performed after the donor mice have established the HGSC-PDX tumors.

***Aims*: #2: Determine the mechanisms by which rAb-anti-CD5L reduces resistance to anti-VEGF therapy in endothelial cells. *Study Design*:**

Major task 2a-2d: We have ordered all the reagents as listed below (Table 1). We will perform the proposed studies once we finish the animal experiments in Aim #1.

Major task 2a. Characterize the cell membrane receptors for stromal CD5L.

Figure 6. Expression of CD36 in the immune components of in HGSC. To decipher the contribution of CD36 expressed in addition to endothelial cells, we've analyzed 19 high-grade serous ovarian cancer (HGSC) samples using single cell RNA sequencing of six populations including T cells, monocytes, epithelial cells, fibroblasts, natural killer cells and B cells. These samples include 4 from the omental metastatic sites, 14 from the primary sites, and 1 normal ovarian sample. We determined the expression of CD5L's membrane-associated receptor, CD36 in the tumor stromal components in these HGSC tumors. First, we found that the expression of CD36 is significantly elevated in tumors including omental metastatic and primary sites in comparison with the normal ovary (**Figure 6A**). Given CD36 is known to express on platelet surface and serves as a receptor for thrombospondin(Yesner, Huh et al. 1996), it is not surprising for us to identify a high level of CD36 expressed in myeloid cells in HGSC tumors (**Figure 6B**). However, it is also noteworthy that our data showed that the C26_stromal clusters containing proliferative endothelial cells (**Figure 6C)** has high expression of CD36, in comparison with myofibroblast cells (C0-myCAF), antigen-presenting cancer-associated fibroblasts (C1-apCAF), and inflammatory CAFs (C4-iCAF) (**Figure 6D).** Collectively, our single-cell studies indicate that the CD5L/CD36 axis is preferentially expressed in the endothelial cells of HGSC tumors.

Figure 6. **Preferential CD36 expression in the TME of high-grade serous ovarian carcinoma.** Freshly resected HGSC tumors (primary tumor and omental metastasis) and 1 normal ovarian sample were collected. (A) Violin plot shows elevated CD36 expression in primary and omental metastatic tumors across all cell types in comparison with normal sample. (B) Violin plot shows the CD36 expression in different cell populations. The expression level across all the epithelial clusters is low, while the myeloid and stromal cells express high-level of CD36. (C) Violin plot showing the expression of CD36 in each myeloid cluster. Clusters 10 and 27 have the highest expression levels of CD36 compared with other clusters. C26-stromal cluster contains proliferative endothelial cells. (D) Violin plot showing the expression of CD36 in stromal cell populations. Clusters 2 showed the highest expression level of CD36 among all the stromal clusters

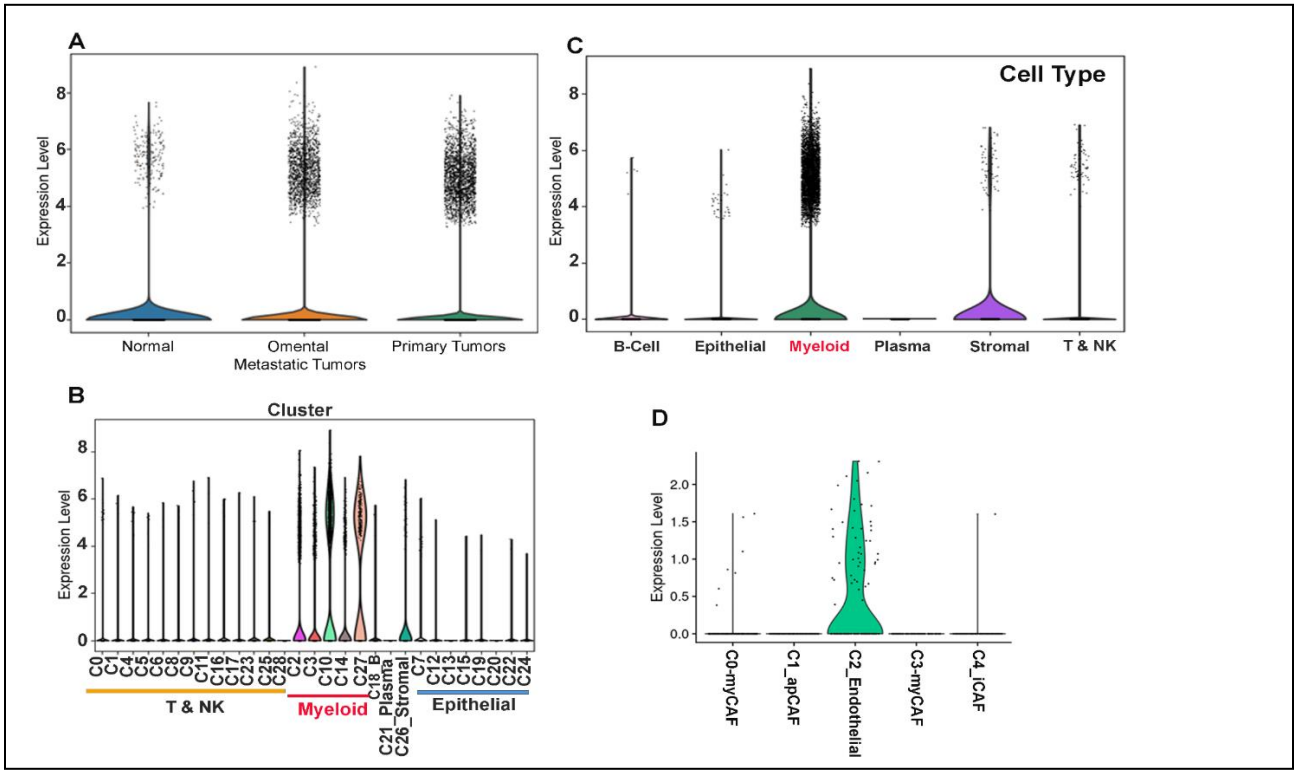

Major task 2b: Identify upstream TFs for up-regulating CD5L mediated endothelial signaling, which promotes the resistance to AVA therapy.

To investigate the mechanisms underlying CD5L overexpression in endothelial cells and the inhibitory effects of rAb-anti-CD5L, we first validated the expression of the previously reported CD5L membrane-associated receptors (CD36, CD5, CD55, and CD59 (Silverstein and Febbraio 2009, Maehara, Arai et al. 2014)) in HUVEC-RF24 cells and in mouse ovary endothelial cells (MOEC). CD36 was more highly expressed than the other receptors in both MOEC and RF24 cells **(Fig. 7**) We next targeted CD36 and CD5 with individual siRNAs and functionally characterized these receptors' roles in CD5L-mediated angiogenic activity in both MOEC and RF24 cells (**Fig 8**). We further performed integrated analysis of the upstream transcriptional factors (TFs) that regulate CD5L expression using Networker 2.0. We discovered that SREBF1 and c-JUN are the TFs responsible for CD5L upregulation during the development of anti-AVA resistance in ovarian cancer patients (**Data pending**). In summary, we successfully characterized the role of endothelial CD5L during the development of AVA resistance. Our results indicated that , along with the emergence of adaptive resistance, local tumor hypoxia leads to increased CD5L secretion by upstream TFs, including PPARγ or SREBF1, which in turn upregulates expression of CD5L, followed by CD5L binding to the membrane-associated receptors including CD36 and CD5, causing activation of the AKT pathway, and leading ultimately to increased cell proliferation and angiogenesis **(Fig 9)**.

In summary, results from this award have laid a solid foundation for us to build a comprehensive understanding of tumor stromal CD5L and its associated membrane-receptor(s) function in endothelial cells, in addition to the existing knowledge of their functions on macrophages. Most importantly, this grant has generated and validated the first monoclonal antibody against CD5L designed to reverse adaptive resistance to AVA therapy. The implications of this outcome for ovarian cancer treatment are substantial and would result in a profound change in the way ovarian cancer patients are treated.

Figure 7. Expression of other membrane receptors for stromal CD5L including CD36, CD55, CD59, and CD5 in endothelial cells. (Left) Mouse ovary endothelial cells (MOEC) and (Right) HUVEC-RF24 cells were fractionated into membrane, cytoplasmic, and nuclear fractions. All fractions and whole lysates were subjected to Western blotting with each membrane-associated receptor.

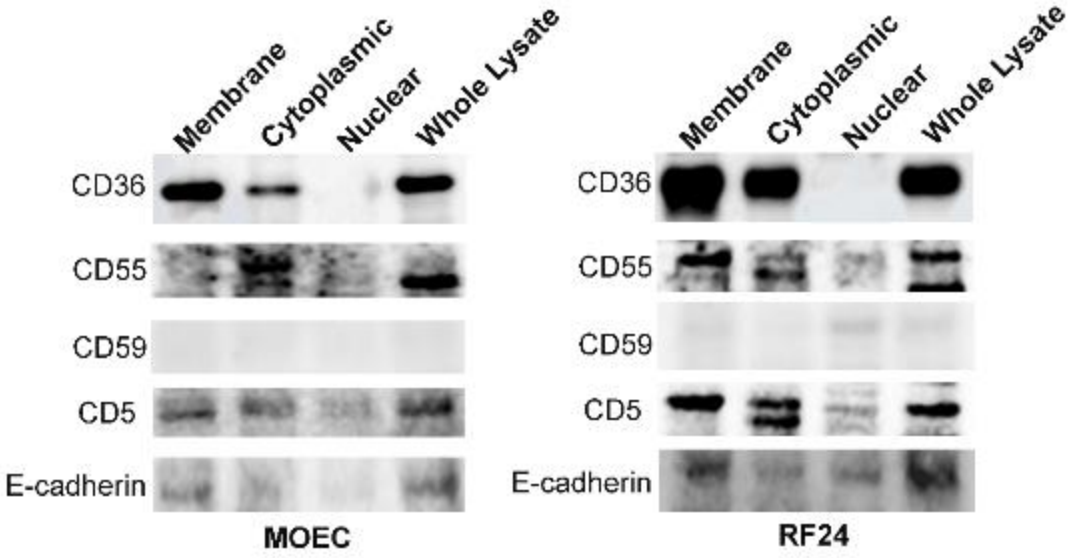

Figure 8. Characterize the roles of cell-membrane receptors CD36 and CD5 on mediating CD5L-stimulated angiogenic events including migration and proliferation. A) Representative images show siRNAs knockdown of CD36 or CD5 expression in RF24 cells reduced the migrated cells in response to CD5L stimulation. (B) Percentage of EdU+ proliferative RF24 cells was significantly reduced upon CD36 or CD5 siRNA knockdown.

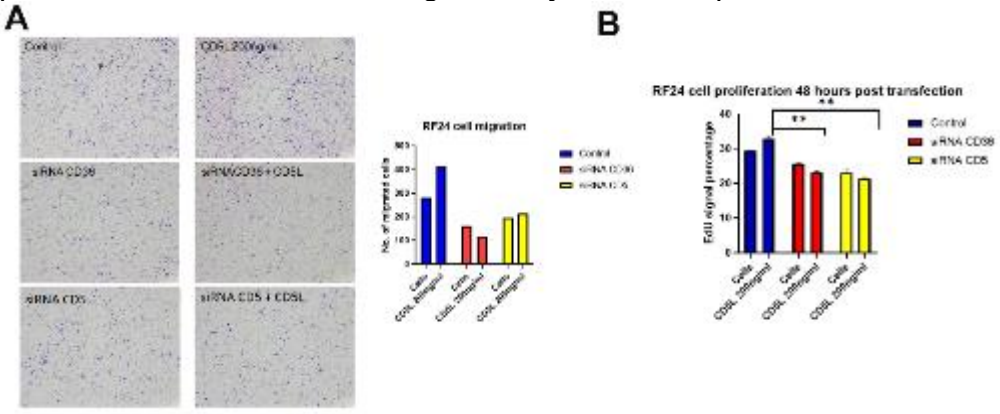

Other studies including tube formation and angiogenic array to investigate the effects of siRNA knockdown of CD36 or CD5 in CD5L stimulated angiogenic events are ongoing.

Figure 9. Mechanism of CD5L-mediated AVA resistance.

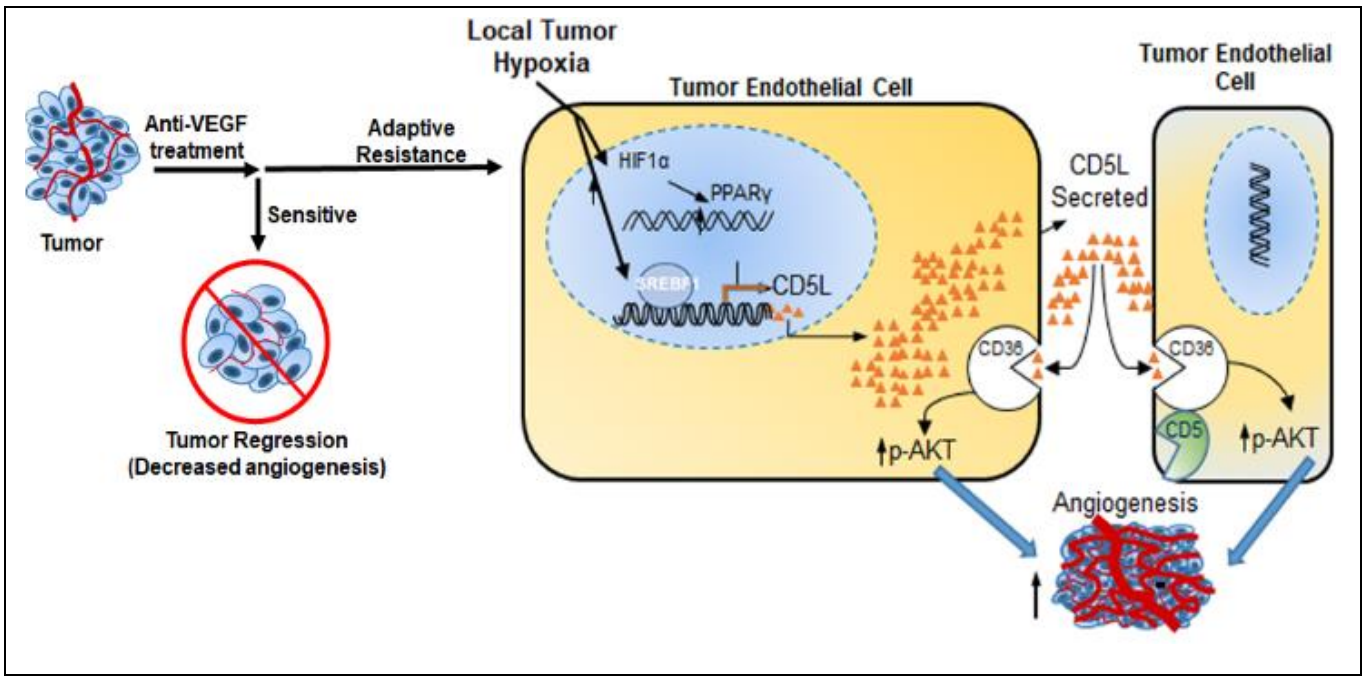

Impact

Although a portion of the molecular pathway leading to anti-VEGF resistance has been reported in the literature, our laboratory is committed to mechanistically characterizing the molecular pathways underlying the development of adaptive resistance to anti-angiogenic therapy, as well as to developing novel therapeutic strategies for the treatment of ovarian cancer with such resistances. Our proposed experiments below will lead to a complete understanding of all upstream and downstream components of CD5L as well as its associated receptor(s). Most importantly, our proposal plans to generate and validate the first monoclonal antibody against CD5L designed to reverse adaptive resistance to anti-VEGF therapy. The implications of this on ovarian cancer treatment are substantial and would result in a profound change in the way ovarian cancer patients are treated.

Changes/Problems

Nothing to report.

Products

Related publications/manuscripts from this grant:

Peer-reviewed Publications:

1. **Wen Y* (*Corresponding author),** Wang Y, Chelariu- Raicu A, Stur E, Liu Y, Corvigno S, Bartsch FJ, Redfern L, Zand B, Kang Y, Liu JS, Baggerly K, Sood AK "Blockade of the short-form of prolactin receptor induces FOXO3a/EIF-4EBP1–mediated cell death in uterine cancer" ***Molecular Cancer Therapeutics***, 2020 Jul 31: PMID: 32737156

2. **Wen Y* (*Corresponding author),** Chelariu- Raicu A, Stur W, Nick AM, Jiang D, Chen X, Lingegowda-Selanere M, Lopez-Berestein G, HungMC, Sood AK "Endothelial p130cas confers resistance to anti-angiogenesis therapy" Cell, Cell Rep. 2022 Jan 25;38(4):110301. doi: 10.1016/j.celrep.2022.110301. PMID: 35081345

3. LaFargue CJ, Amero P, Noh K, Lingegowda SM, **Wen Y(*Corresponding author),** Pradeep S, Wan Yh, Yoo W, Bayraktar E, Dasari SK, Vathipadiekal V, Chelariu-Raicu V, Roopaimoole R, Ku ZQ, Hui D, Xiong W, Choi HJ, Ali-Fehmi R, Lu C, Birrer MJ, Hu W, Zhang NY, Lopez-Berestein G, Franciscis V, An ZQ, Sood AK*(*Corresponding author)* "Overcoming Adaptive Resistance to Anti-VEGF Therapy by Targeting CD5L" **Nature Communication**. 2023 Apr 26;14(1):2407. PMID: 37100807.

Participants & Other Collaborating Organizations

Drs. Ningyan Zhang and An Zhiqiang at the University of Texas Health Science Center at Houston

Special Reporting Requirements

Nothing to report.

Appendices

Nothing to report.

References:

Chen, J. (2012). "Regulation of tumor initiation and metastatic progression by Eph receptor tyrosine kinases." Adv Cancer Res 114: 1-20.

Maehara, N., S. Arai, M. Mori, Y. Iwamura, J. Kurokawa, T. Kai, S. Kusunoki, K. Taniguchi, K. Ikeda, O. Ohara, K. I. Yamamura and T. Miyazaki (2014). "Circulating AIM prevents hepatocellular carcinoma through complement activation." Cell Rep 9(1): 61-74.

Silverstein, R. L. and M. Febbraio (2009). "CD36, a scavenger receptor involved in immunity, metabolism, angiogenesis, and behavior." Sci Signal 2(72): re3.

Yesner, L. M., H. Y. Huh, S. F. Pearce and R. L. Silverstein (1996). "Regulation of monocyte CD36 and thrombospondin-1 expression by soluble mediators." Arterioscler Thromb Vasc Biol 16(8): 1019-1025.